Aqueous tert-butanol mixtures: A model for molecular-emulsions

Bernarda Kežić and Aurélien Perera

Citation: J. Chem. Phys. **137**, 014501 (2012); doi: 10.1063/1.4730524
View online: http://dx.doi.org/10.1063/1.4730524
View Table of Contents: http://jcp.aip.org/resource/1/JCPSA6/v137/i1
Published by the American Institute of Physics.

Aqueous *tert*-butanol mixtures: A model for molecular-emulsions

Bernarda Kežić[1,2] and Aurélien Perera[1]
[1]*Laboratoire de Physique Théorique de la Matière Condensée (UMR CNRS 7600), Université Pierre et Marie Curie, 4 Place Jussieu, F75252 Paris cedex 05, France*
[2]*Department of Physics, Faculty of Sciences, University of Split, Nikole Tesle 12, 21000 Split, Croatia*

(Received 17 April 2012; accepted 7 June 2012; published online 2 July 2012)

By analogy with micro-emulsion, we introduce the molecular-emulsion picture to describe particular aqueous mixtures. The analogy is set by introducing the equivalent of the Teubner-Strey structure factor, the latter which is traditionally used to describe the structure of micro-emulsions. The main difference resides in the fact that the size of the oil and water domains are not in the micrometer, but in the nanometer scale. This implies that the molecular size and the molecular geometry cannot be neglected anymore. The introduction of this analogy is used to settle the problem of properly describing with computer simulations highly micro-heterogeneous aqueous mixtures. In particular, the issue of whether or not the Kirkwood-Buff integrals represent solely concentration fluctuations is settled by showing the contribution of the micro-heterogeneity to these integrals through the presence of an associated pre-peak in the structure factors. Both the Optimized Potentials for Liquid State (OPLS) and Transferable Potential for Phase Equilibria–United Atoms (TraPPE-UA) force fields for *tert*-butanol turn out to be remarkably good in describing the structure of the corresponding aqueous mixtures, when the above-mentioned analogy with micro-emulsion is introduced to correct for the computational artifacts in the Kirkwood-Buff integrals. © *2012 American Institute of Physics*. [http://dx.doi.org/10.1063/1.4730524]

I. INTRODUCTION

Micro-emulsion (ME) has been a wide subject of interest in the 1980s, for a community including chemists, physical-chemists and physicists.[1–4] The microscopic structure of these mixtures has remained elusive until Teubner and Strey (TS) introduced a fit for the experimentally observed neutron scattering intensities.[5] Their fit was based on a Landau-Ginzburg free-energy Hamiltonian expansion in term of local density,[6] and the outcome of this study showed that 2 lengthscales were sufficient to describe the scattering intensities, the domain-size parameter d, and the concentration fluctuation length ξ. This TS fitting expression, that we recall in Sec. II, allowed to unify in a single expression, scattered intensities corresponding to a wide range of microscopic structures, from the disordered ME phase up to micellar or lamellar phases.[7] In this phenomenological expression, although microscopic parameters such as the domain size or correlation length are introduced, the underlying molecular level microscopic picture is entirely missing. Even though various lattice-based theories were introduced later on,[4] it was found that the molecular level description is never really needed to give a qualitative picture of these systems. This is even true in recent computer simulations of micelle forming systems[8] that use coarse grained molecules, in order to avoid excessive computational resources. One possible explanation for the absence of needing a detailed molecular picture lies in the fact that the different mesoscopic objects (oil-water domains, micelles, etc.) can be described as continuous fields, since their extent is much larger than the molecular sizes. One can naturally doubt that the validity of such phenomenological approach remains valid when the domain sizes become comparable to the molecular sizes.

Micro-emulsions are essentially aqueous mixtures, where the main solute is of the oil-type and surfactant molecules help stabilize the interfaces by sitting between the water and oil domains, since they are bipartite molecules.[1] A simplified ME is a mixture of water and surfactant molecules, where the surfactant must have a rather large oily tail. In such mixture, the tails segregate from the water domains and form the oil domains, with the polar heads sitting at the interface.[9,10] Large alcohol molecules such as 2-butoxy-ethanol are about the minimal size required to form lower end micro-emulsions.[10] When it comes down to even smaller alcohol molecules, such as 1-propanol, *tert*-butanol (TBA), ethanol, or methanol, one can hardly consider the corresponding aqueous mixtures as micro-emulsions, since the water and oil domains are about the nanometer size, and the granularity of the molecules cannot be neglected anymore. In such a mixture, the mesoscopic concept of interface disappears, even though domains can be clearly seen. Indeed, it is now well-known that even in the case of aqueous methanol mixtures, molecular dynamics simulations show strong micro-heterogeneity, with clear micro-segregation of water and methanol domains.[11–13] In fact, any solute molecule that has methyl groups together with a hydrogen bonding group is likely to show such micro-segregation. We suggest that such mixtures should be termed "molecular emulsions" (mE), since the word nano-emulsions is already taken to describe emulsions that form nano-droplets in a non-equilibrium context.[14]

This micro-heterogeneity, characterized by the labile formation of nano-meter sized domains of water and solute

molecules, evolves at the scale of the nanosecond, while underlying molecules evolve at the scale of the pico-second. Hence, it has been noted by several authors[15–18] that this situation requires the need of large scale simulations, mostly beyond $N = 1000$ particles, as well as run lengths of the order of several nanoseconds, in order to sample properly both the molecular scale and the domain scale dynamics. This brings us to the heart of the matter. It was noted by some authors that most of the existing force fields for the solute molecule, in particular the OPLS force fields, were not adapted to describe the formation of micro-heterogeneity (MH). Indeed, the distribution functions computed from such force fields exhibit a pathological long range behaviour that leads to Kirkwood-Buff integrals (KBIs) several times larger than the experimental values. It was equally noted that, even with systems of $N = 2000 - 3000$ particles, it was not possible to unambiguously stabilise the long range part of the distribution functions. Some authors have proposed to modify the force fields in order to have the asymptote of the correlation function to match the experimental values of the KBIs within large but computationally reasonable system sizes.[15–17] This was suggested in the case of the acetone models,[16] for which such modification did lead to smaller domain sizes, hence avoiding the demixing tendency observed for the case of the OPLS acetone model.[18] It is not obvious that this procedure would not in fact modify the "true" micro-segregation to adapt it to smaller scales. To date, the exact relation between the existence of nanoscale segregated domains, the asymptotical behaviour of the correlation function, and the molecular force fields, is largely unknown from rigorous statistical physics grounds.

The aim of this article is to palliate for this situation by invoking a formal analogy between micro-emulsions and molecular-emulsions, on the basis of the specific form of the structure factor,[5] by adapting it across scale of 3 orders of magnitude. Instead of modifying the force fields in order to scale the correlations within a given box size, we propose to modify the calculated correlation functions in their long range part, in order to obtain a correct asymptotical behaviour. The rationale behind this procedure is that the micro-heterogeneity is not properly scaled within the simulation box, and therefore it distorts the asymptote of the correlations. Instead of performing larger, but more expensive simulations, we undistort the asymptotes according to a model – that of the structural analogy between the ME and the mE. The success of this operation will be justified if reasonable KBIs are obtained. To illustrate this procedure, we use here the SPC/E water[19] and two force fields for TBA, the OPLS force field,[20] and the TraPPE-UA force field[21] – both for which excessively large KBIs are obtained from the simulations, and we show here that our procedure leads to KBI in better agreement with known experimental values than what is obtained from the original simulations. It is noteworthy that not all aqueous mixtures require such corrections. In particular, correlations in aqueous mixtures of small alcohol molecules such as methanol or ethanol can be studied reliably with current force fields and computer simulations about 2000 particles, provided other essential corrections to the asymptotical form of the correlations are taken into account. We address this important point in Secs. II E and II F. In particular, improving the force fields in order to recover the proper KBIs for systems such as aqueous methanol[16] is not the issue that we address here.

The aqueous-TBA mixtures have been long recognized to have some pronounced aggregative structure and have attracted the attention of experimentalists and simulators.[22–26] Detailed investigation of the structure has been made through neutron scattering,[12] focussing on low and high TBA regions for this latter,[27,28] as well as x-ray scattering.[30] The recent computer simulations of Lee and van der Vegt[17] revisit the force field of TBA in order to reproduce the micro-structure of the mixture that previous models seem to overestimate. In this work, we will address precisely the topic of the micro-segregated structure of this mixture that seems to be particularly suited for such a study.

The outline of the paper is as follows. First, we recall the statistical mechanics related to liquid state theory that may help to justify the analogy made here between ME and mE, as well as the details about the TS approach and the molecular dynamics simulations. In Sec. III we describe the correlations and the methodology as well as results for the KBI. Finally, the conclusions about the merits and limits of the present approach are detailed.

II. THEORETICAL CONSIDERATIONS

The TS approach to micro-emulsions[5] is based on field theoretic techniques which have a phenomenological basis, much like the van der Waals approach to the liquid-gas coexistence. A true microscopic theory should start from liquid state statistical considerations. We sketch here such an approach.

A. Teubner-Strey approach to micro-emulsions

Teubner and Strey considered field theoretic approaches to deduce the form of the asymptotic behaviour of the scattered intensity $I(q)$, where q is modulus of the wave vector. In this approach, the microscopic order parameter is the density $\phi(r)$. This quantity depends only on the distance r, and describes the general distribution of matter by neglecting molecular details. Since the Fourier transform of the gradient $\vec{\nabla}\phi(r)$ is $i\vec{q}\hat{\phi}(q)$, one can write the free-energy Hamiltonian in terms of multiple gradients operators of the density and obtain a polynomial of q^2 in the Fourier space. Retaining terms up to $\hat{\phi}^4$, then minimising the free-energy Hamiltonian in order to get solutions for equilibrium conditions, one constructs a pair correlation function as $<\phi(q)\phi(0)>$. From the corresponding structure factor one obtains the following form for the scattered intensity:[5]

$$I(q) \approx \frac{I(0)}{a + q^2 c_1 + q^4 c_2}.$$

B. Teubner-Strey approach to molecular-emulsions

The equation above can be rederived from the standard liquid state theory through the molecular Ornstein-Zernike equation (MOZ). This theory deals with the pair correlation function $h(1, 2)$ and the direct correlation function $c(1, 2)$,

between molecules 1 and 2. These functions can be expanded on a basis of rotational invariants, in order to separate the angular variables from the radial part.[31]

For a one component liquid, this equation reads in matricial form as

$$\tilde{H}_\chi(q) = \tilde{C}_\chi(q)[I - (-)^\chi \rho \tilde{C}^\dagger_\chi(q)]^{-1}, \quad (1)$$

where ρ is the density, and the matrices indexed by χ have for elements the projections of the pair and direct correlation functions in Fourier-Hankel space, on a basis of rotational invariants.[31] For a system of axio-symmetric molecules the relations would be $\tilde{A}_{mn} = \{\tilde{A}_\chi(q)\}_{mn} = \tilde{a}_{mn\chi}(q)$, where $\tilde{A} = \tilde{H}, \tilde{C}$, and $\tilde{a}_{mn\chi}(q)$ is the Fourier transform of the correlation function $a_{mn\chi}(r)$ with $a = h, c$, the pair and direct correlation functions, respectively. For more complex molecular geometry, more indices come into play and the matrix elements must be redefined accordingly. The matrix $\tilde{C}^\dagger$ is a simple transform of the $\tilde{C}$ matrix that changes the sign of indexing variables that appear in the expansion of the correlation functions in terms of rotational invariants.[32] The details of how the matrix elements $a_{mn\chi}$ are related to the full correlation function $a(1, 2)$ has been explained in several articles[32,33] and is now textbook knowledge.[34] In particular, it is important to recall that the $\tilde{a}_{mn\chi}(q)$ are in fact what is called a χ −transform involving projections $\tilde{a}^{mnl}(q)$ each of which are Fourier-Hankel transforms of order l of the functions $a^{mnl}(r)$.[32]

The matrix equation Eq. (1) can also be written for a mixture, and looks just the same, except that the (m, n) indexing is more complicated since each matrix A is now a block matrix where each block is a submatrix with elements being correlation functions $a_{ij}(1, 2)$ corresponding to pair of species (i, j). The mathematics of the MOZ that concern the present development are really simple.[33] To illustrate the method, we will use the example of axio-symmetric molecules. We wish to examine the behaviour at small-q of any $\tilde{h}_{ij;mn\chi}(q)$. In order to achieve that, one has to compute the inverse of the matrix $\tilde{D}(q) = [I - (-)^\chi \rho \tilde{C}^\dagger_\chi(q)]$ in MOZ. This will make the determinant to appear in the denominator expression for $\tilde{h}_{ij;mn\chi}(q)$. This determinant can be written in short as $1 - \tilde{\gamma}_\chi(q)$, where the relation between the new function $\tilde{\gamma}_\chi(q)$ and the matrix $\tilde{C}_\chi(q)$ will be a complicated algebraic expression involving all of the $\tilde{c}_{ij;mn\chi}(q)$ functions and their various products. What is important to notice is that *all* $\tilde{h}_{ij;mn\chi}(q)$ will have the *same* denominator $1 - \tilde{\gamma}_\chi(q)$. In short, one has, from MOZ

$$\tilde{h}_{ij;mn\chi}(q) = \frac{\tilde{t}_{ij;mn\chi}(q)}{1 - \tilde{\gamma}_\chi(q)},$$

where the function in the numerator is related to the matricial product of $\tilde{C}_\chi(q)$ to $\tilde{D}(q)$. The details of these calculations are not relevant to the argument, since the general form above is exactly equivalent to MOZ, and holds for complex molecular geometries. Since the function $\gamma_\chi(r)$ involves only direct correlation functions, which are short ranged functions, one can expand this function around $q = 0$, and one has

$$\tilde{h}_{ij;mn\chi}(q \to 0) \approx \frac{\tilde{t}_{ij;mn\chi}(0)}{1 - \tilde{\gamma}_{\chi;0} - q^2\tilde{\gamma}_{\chi;2} - q^4\tilde{\gamma}_{\chi;4} - q^6\tilde{\gamma}_{\chi;6} - \ldots},$$

where only even powers of q are retained because of the general symmetry of all correlation functions $a(-r) = a(r)$. The small-q expansion involves expanding Fourier-Hankel transforms and it is not so simple to express each of the $\tilde{\gamma}_{\chi;n}$ in terms of integrals of the $\gamma_\chi(r)$ function, as it would have been in case of a simple Fourier transform. But this is a minor detail irrelevant to the generality of the discussion here. The equation above retained to order q^2 alone will lead to the well-known discussion in terms of the correlation length.[35] We briefly recall this argument here

$$\tilde{h}_{ij;mn\chi}(q \to 0) \approx \frac{\tilde{t}_{ij;mn\chi}(0)}{1 - \tilde{\gamma}_{\chi;0} - q^2\tilde{\gamma}_{\chi;2}} = \frac{A_{ij;mn\chi}}{\xi^{-2} + q^2}, \quad (2)$$

with ξ the correlation length expressed as $\xi = \sqrt{-\tilde{\gamma}_{\chi;2}/(1 - \tilde{\gamma}_{\chi;0})}$. This function is seen to be a Lorentzian, and its inverse Fourier transform is a Yukawa function,

$$\lim_{r\to\infty} h_{ij;mn\chi}(r) \approx A_{ij;mn\chi}\frac{\exp(-r/\xi)}{r}. \quad (3)$$

It is important to note that there is a unique correlation length ξ that is the same for all projections. In fact, a more detailed analysis shows that the correlation length is specific to the projections associated to the projections that contribute to the mechanical stability of the system.[36] We will not get into such details herein since these do not affect the generic form in Eqs. (2) and (3).

The correlation length is sensitive to density fluctuations in a pure liquid or concentration fluctuations in a mixture. In particular, it is a very useful probe of the approach of any global phase transition regions, since fluctuations are enhanced in their vicinity, hence the correlation length tends to increase and diverge at the limit of stability of the phase – the so-called spinodal. But what happens when the system does not phase separate in global fashion and only micro-segregates, like in all alcohol water mixtures? In order to study such phenomenon, one should retain one more order in the q-expansion, which amounts to explore distances shorter than the domains of critical fluctuations which are of several tens of Angstroms. In principle, there should be no reason to stop the expansion at q^4 or q^6. However, since the expansion at q^4 has been successfully used from micro-emulsions down to aqueous mixtures of relatively short chain alcohol molecules, such as diols, triols, and others,[9,10] there are good reasons to try the TS approximation first.

The molecular level TS equivalent of the MOZ equation amounts to retaining higher order terms in q,

$$\tilde{h}^{(TS)}_{ij;mn\chi}(q) = \frac{\tilde{t}_{ij;mn\chi}(0)}{1 - \tilde{\gamma}_{\chi;0} - q^2\tilde{\gamma}_{\chi;2} - q^4\tilde{\gamma}_{\chi;4}} = \frac{\tilde{t}_{ij;mn\chi}(0)}{a_2 + q^2c_1 + q^4c_2},$$

where we have adopted the original TS notation[5] in the denominator of the second equality, and where the new coefficients can be redefined in terms of the domain size d and the correlation length ξ as follows:[5,41]

$$a_2 = 1 - \tilde{\gamma}_{\chi;0} = (\bar{d}^2 + \xi^2)^2,$$

$$c_1 = -\tilde{\gamma}_{\chi;2} = 2(\bar{d}\xi)^2(\bar{d}^2 - \xi^2),$$

$$c_2 = -\tilde{\gamma}_{\chi;4} = (\bar{d}\xi)^4,$$

where $\bar{d} = d/2\pi$. The second equalities introduce the two length scales $(\bar{d}, \xi)$ that allow to write the inverse Fourier transform of the TS function in the following compact form:

$$h^{(TS)}_{ij;mn\chi}(r) = \int d\vec{q}\ \exp(i\vec{q}.\vec{r})\, \tilde{h}^{(TS)}_{ij;mn\chi}(q) = \frac{\tilde{t}_{ij;mn\chi}(0)}{\pi^2(\bar{d}\xi)^3}\, \frac{\exp(-r/\xi)}{r} \sin(r/\bar{d}).$$

One sees that the relations between the 3 TS coefficients (a_2, c_1, c_3) and the combinations of length parameters $(\bar{d}, \xi)$ are stringent, since the moments of the $\gamma_\chi(r)$ functions need to have specific signs to match the algebraic forms and the positivity conditions. Since these functions cannot be obtained unless one calculates the direct correlation function expansion coefficients, this information is unavailable to us. The obtention of such coefficients needs the arsenal of liquid state theory, and reliable output from such theory for realistic molecular system is not well developed at present. Therefore, in our approach to strong micro-heterogeneous systems, we will test the TS functional form to correlation functions determined by computer simulations. However, the implementation of this method to simulation results poses certain problems that we discuss in Sec. III.

C. Molecular dynamics simulations

We have used SPC/E model[19] for water and two models for TBA, the OPLS model,[20] and the newer TraPPE-UA model.[21] Molecular dynamics simulations in the constant NPT isobaric ensemble were performed, with a total of $N = 2048$ molecules, for the ambient conditions of temperature (T = 300 K) and pressure ($p = 1$ atm) by using the DL_POLY2 program.[37] Ewald summations were used to account for the partial charges in periodic conditions. The time step for the integration of motion was fixed at 2×10^{-15} s in all the calculations, which was found in our previous works satisfactory in order to reproduce the rotational motion of water. Mole fractions steps of 0.1 were used to study the whole range of mixtures and $x = 0.05$ was equally studied. The TraPPE-UA model was studied for less concentrations since we were interested in the differences between the two models for cases where the micro-heterogeneity is very different. Each concentration was initially randomly generated in a box whose volume was approximately set to the experimental one, and were equilibrated initially in the constant NVT conditions for 100 ps with all partial charges set to zero, in order to have a homogeneous mixture without the micro-segregation set by the presence of these charges. Then the charges were turned on to their model values and the system further equilibrated for 200 ps in constant NVT conditions, in order to avoid brutal volume changes, and then equilibrated in the NPT conditions for time varying from 1 ns to 1.5 ns depending of concentrations. Long equilibrations were needed around $x = 0.1 - 0.3$, where the maximum of concentration fluctuations occur.

D. The micro-heterogeneity in the simulations

For all these concentrations, it was found that, starting from a homogeneous mixture, micro-heterogeneity sets up very fast, within few ps. Then, this MH evolves very slowly, basically by coarsening of the water and alcohol domains, much like what was observed in our previous aqueous systems in general. It is this coarsening process that needs the large simulation times that are in the nanoscale range. This is already a leading information about the kinetics of these systems: the time scale at which the MH evolves is 2–3 orders of magnitude that of the molecular scales. So, most the simulation times are spent probing the various conformation of the MH inside the simulation box, and these conformations may never reach a true equilibrium if the "proper" system sizes are not considered. There is no method to know *a priori* which is the right size. The best probe that was empirically found by several authors[15,17,18,43] is the stabilisation of the asymptote of the running Kirkwood-Buff integral (RKBI) the latter which are defined as

$$G_{ab}(R) = 4\pi \int_0^R dr\, r^2 (g_{ab}(r) - 1), \tag{4}$$

for each pair of species (*a,b*), where $g_{ab}(r)$ is the radial distribution function (RDF) between the centers of mass of the 2 molecules belonging to species a and b. Since the center of the correlations is arbitrary, the Kirkwood-Buff integrals defined as the limit of the RKBI

$$G_{ab} = \lim_{R\to\infty} G_{ab}(R)$$

is independent of the choice of the molecular center, and therefore any pairs of sites (a, b) residing of each the molecular species can be used for this calculation. These asymptotes tend to vary from one run to another, even across 1 nanosecond, because the morphology of the MH evolves at this time scale. For example, in the equimolar aqueous-methanol systems, one cannot stabilise the asymptote of $G_{ww}(r)$ even after very long runs of several nanoseconds,[38] and this asymptote is seen to oscillate around some value G_{ab} which is nevertheless close to the experimental value. For the present system, we could not even reach a stable asymptote for some concentrations around $x = 0.1 - 0.3$, where the experimental concentration fluctuations are very large.[30] For a system of $N = 2048$, one reaches values of the KBIs that are 3–4 times the experimental ones. This type of behaviour proves that either the system sizes are still too small, or that the OPLS force field is not good, the latter which was considered in Ref. 17.

Before we examine the results of our calculations, we need to look at one more problem posed by the determination of correlation functions in finite size simulations.

E. Exact asymptote of the pair correlation function in liquids

As we have stated in a recent work,[38] the asymptote of the various correlation functions that are calculated by computer simulations is marked by the fact that their asymptote is not one, as it should be, but a value that depends on the system size and the fluctuations of the system. This result has been established decades ago by Lebowitz and Percus.[39] Their

result, extended to mixtures, can be written as

$$\lim_{r\to\infty} g_{ab}(1,2) = \lim_{r\to\infty} g_{i_a j_b}(r) = 1 - \frac{1}{N\sqrt{x_a x_b}} \frac{1}{\rho_b} \left(\frac{\partial \rho_a}{\partial \beta \mu_b}\right)_{T N_k}, \quad (5)$$

where μ_a, ρ_a, and x_a are, respectively, the chemical potential, density, and mole fraction of species a, $\beta = 1/k_B T$ is the Boltzman factor and N the number of particles, and the partial derivative is taken while keeping T and the number of particles N_k other than species (a, b) constant. The second equality in Eq. (5) states that the asymptote is the same for any site–site correlation function between sites (i_a, j_b) on molecules of species (a, b), respectively. In the limit of very large system sizes the exact limit is obtained. It is important to note that this limit is incorrectly written in many works and the partial derivative term is entirely ignored. This would be correct only for non-interacting ideal gas system. The existence of such a limit can be spotted out by zooming on the asymptote of the correlation functions obtained in computer simulations. One observes in all cases a small shift of the asymptote under the unity asymptote, and it is easy to verify that this cannot be corrected by simply adding $1/N$. Neglecting to correct for this error leads to RKBIs that have a systematic cubic downward curvature because of the non-cancellation of the integrand in Eq. (4) at large distances.

One cannot compute the chemical potential in a computer simulation in such a reliable and accurate manner as to extract a proper density derivative. In order to remedy for this problem, we have proposed in a recent work an empirical procedure to shift the asymptote to unity without affecting the correlation functions in the range of the first few neighbours. The corrected site–site correlation functions between sites (i, j) belonging to 2 species (a, b) are calculated as

$$g_{ij}^{(corrected)}(r) = g_{ij}(r)[1 + (1 - \alpha_{ij}) S_{ij}(r)],$$

where α_{ij} is the wrong asymptote of $g_{ij}(r)$, and $S_{ij}(r) = \frac{1}{2}[1 + \tanh(\frac{r-\kappa_{ij}}{\theta_{ij}}))]$ is the switch function that smoothly brings the incorrect asymptote limit α_{ij} to unity. The parameters $(\kappa_{ij}, \theta_{ij})$ must be fitted in order to achieve this properly. In practice, we choose $\kappa_{ij} = \sigma_{ij}$, where σ_{ij} is the largest distance at which $g_{ij}(r) \neq 0$, which is roughly a contact distance between sites i and j, and this choice ensures that the part of the correlation function for $r < \kappa_{ij}$ corresponding to the first 2 peaks is not affected by the transformation, and we choose $\theta_{ij} = 1$ which ensures a smooth change of the step function $S_{ij}(r)$. Example of application of this procedure have been demonstrated in our previous works.[38,40,41] We will refer to this essential correction as the LP correction (LP for Lebowitz-Percus[39]).

F. Methodology of the TS transformation

Once the site–site functions calculated from the simulations have been corrected for the asymptote, there remains in the same asymptotical part the contribution of the MH which, as explained above, is not relaxed in the time and spatial scales at which we sample the correlation functions. It is often seen that the molecular size oscillations are not yet entirely damped at the half-width of the simulation box. Similarly, the domain size oscillations are certainly not damped at the half-width of the box since they are at greater scales. The proper way to handle this problem would be to study truly mesoscopic systems, where one would fix the number of domains instead of the number of molecules. To fix the idea, a typical box size would correspond to $N_m = 256$ "domains," each domain size being about 15 Å, which is the typical size we encounter in our simulations. The number $N_m = 256$ corresponds to typical sizes that were used in earlier simulations of liquids. If we consider that we have about $N = 200 - 300$ molecules per domain on average, that leads to a total of $50 - 75$ thousand molecules. While this is not out of range of the current computational power, it is still in the very high range of our current setups. While one can imagine doing a few such simulations for testing purposes, it is out of the question to study these systems routinely by using such large configurations.

Instead, we choose here to prolongate the incomplete ending in the long range part of the correlations between pair of sites (i, j) belong to species (a, b) by a TS function of the form

$$t_{ij}(r \geq L) = A_{ij} \frac{\exp(-(r - L)/\xi)}{r} \sin((r - R_{ij})/\bar{d}), \quad (6)$$

which applies from the end of the correlation function at the distance corresponding to the half-width L of the simulation box. The parameters (A_{ij}, R_{ij}) are adjusted to match the value $g_{ij}(r = L)$, as well as to keep the derivative continuous at that merging point. The reduced domain size parameter $\bar{d} = d/2\pi$ is matched to the size of the oscillations representing the domains. Finally, the correlation length ξ is set to damp the oscillations quickly, that is after a full period of domain oscillations. These 2 parameters are the same for all site–site correlation functions, independently of the species pairs, according to the theoretical developments of Secs. II A–II E.

We discuss now the choice of these parameters for a given mole fraction. The (A_{ij}, R_{ij}) parameters are fixed by the value of $g_{ij}(r = L)$ and offer no margin of choice. The leading control parameter is the domain size d. The zoomed plot on the tail of $g_{ij}(r)$ always gives a hint on the large scale oscillations, and this is even further enhanced by plotting the RKBI. In all cases we have tried to match the period hinted by these oscillations. This is demonstrated, for example, in Fig. 6 for $x = 0.2$ which is in the region of strong concentration fluctuations (see Sec. III below). The correlation length parameter controls the decay of the oscillations, and this is the only parameter that is really arbitrary in the fit. Unless mesoscopic simulations for these systems are done, it is difficult to estimate the way the correlations decay. Our current guess is based on the guess that the flat asymptote of the RKBI should be reached relatively quickly, that is with at most one full period of oscillation over the MH domain.

We note that the TS extension is needed only for those systems which exibit such strong micro-heterogeneity that it would distort the tail of the correlations at medium range. From our earlier studies, examples of systems not requiring TS extensions are aqueous-methanol[38] and aqueous-ethanol.[40] Both these aqueous mixtures involve alcohol molecules smaller than the present ones. Therefore, the

influence of the solute size, and possibly the size of the hydrophobic groups has some importance in the amplitude of the micro-heterogeneity. We note, however, that in both this latter work we needed to properly implement the LP correction explained in Sec. II E. We equally note that extensions to the correlations in neat systems and mixtures have been proposed earlier by other authors,[42] in view to reproduce the KBI accurately, but these extensions did not address the essential LP corrections.

III. RESULTS FOR AQUEOUS *TERT*-BUTANOL MIXTURES

While aqueous *tert*-butanol mixtures have been previously studied by other authors,[17,21,25,26] the focus of the problems caused by micro-heterogeneity has been addressed only scarcely.[17] From the experimental side, the focus of local structure has primarily been studied by various scattering techniques, light scattering, small angle neutron techniques principally by Soper and collaborators,[12] x-ray scattering by Nishikawa and collaborators.[30] The small TBA concentration region has been a particular focus of attention.[27,48,52] However, we did not investigate this particular case in the present study. On the computer simulations sides, most previous studies are for system sizes too small[25,26] (typically less than 800 molecules) to be conclusive about micro-heterogeneity. All these works underline the presence of micro-heterogeneity. The only work that stands out with respect to this problem is that by Lee and van der Vegt,[17] with system sizes in the range between $N = 1000 - 4000$ molecules. These authors have noticed that former OPLS and GROMOS (Ref. 17) force fields produce excessively large KBIs, and they proposed a new force field based on fitting principally the partial charges, hence the dipole moment, to reduce the KBIs to the experimental values. The reported KBIs are in excellent agreement with some of the experimental values.[17] This proves that one can certainly alter the force fields in order to match the correct KBI, and this methodology has been pursued with great success for various systems.[15,16]

A. Neat *tert*-butanol

Since we have used two different force fields for TBA, it is worthwhile comparing their structural properties. In Fig. 1 we compare some of the typical site–site functions, and there are quite significative differences between the two models. All the other site–site functions are within similar agreement range. Since we use rigid version of both models, there are some differences between the enthalpies and volumes. In particular, we find that the enthalpy of TraPPE-UA TBA is 10 kJ larger than the enthalpy reported in Ref. 21 which is closer to the experimental enthalpy (−47.88 kJ/mol) while the rigid OPLS model gives −47.75 kJ/mol. Both the volumes for OPLS (92.25 cm^3/mol) and TraPPE-UA (97.56 cm^3/mol) force fields agree relatively well with the experimental value (94.91 cm^3/mol).

B. Thermodynamics

In Fig. 2, we show the enthalpies and excess enthalpies (inset) in the upper panel, and the corresponding volumes and excess in the lower panel, both compared with experimental values and results from Ref. 17. As usual the experimental enthalpies must be corrected by a factor $5(1 - x)$ kJ/mol, where x is the mole fraction of TBA, since there is a polarisation effect correction of 5 kJ/mol for pure water.[18,19] In much the same spirit, we have implemented a correction of $-10x$ kJ/mol for the TraPPE-UA model due to the 10 kJ discrepancy with pure TBA. It is seen that the overall agreement is relatively good, confirming that all these classical models are well suited to capture the principal features of these thermodynamical properties. There are, however, appreciable

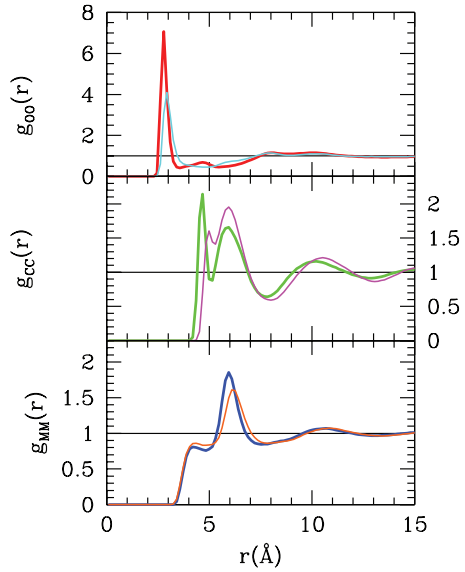

FIG. 1. Comparison of selected site–site RDFs between the neat OPLS (thicker lines) and TraPPE-UA (thinner line) models. Top panel for oxygen–oxygen, middle panel for carbon–carbon, and bottom for methyl–methyl site–site RDFs.

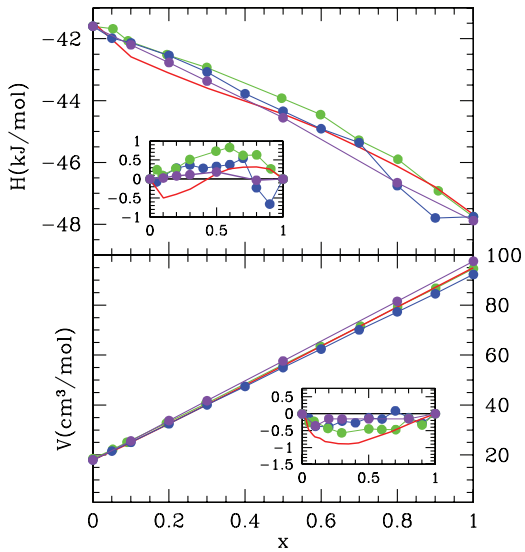

FIG. 2. Enthalpies (top panel) and volumes (lower panel) for the aqueous TBA mixtures as function of the TBA mole fraction. Insets: corresponding excess quantities. Red lines for expt. data, enthalpies from Ref. 50 and volumes from Ref. 51, green dots are simulation results from Ref. 17, blue dots for OPLS TBA and purple dots for TraPPE-UA TBA. Lines connecting the dots are guidelines.

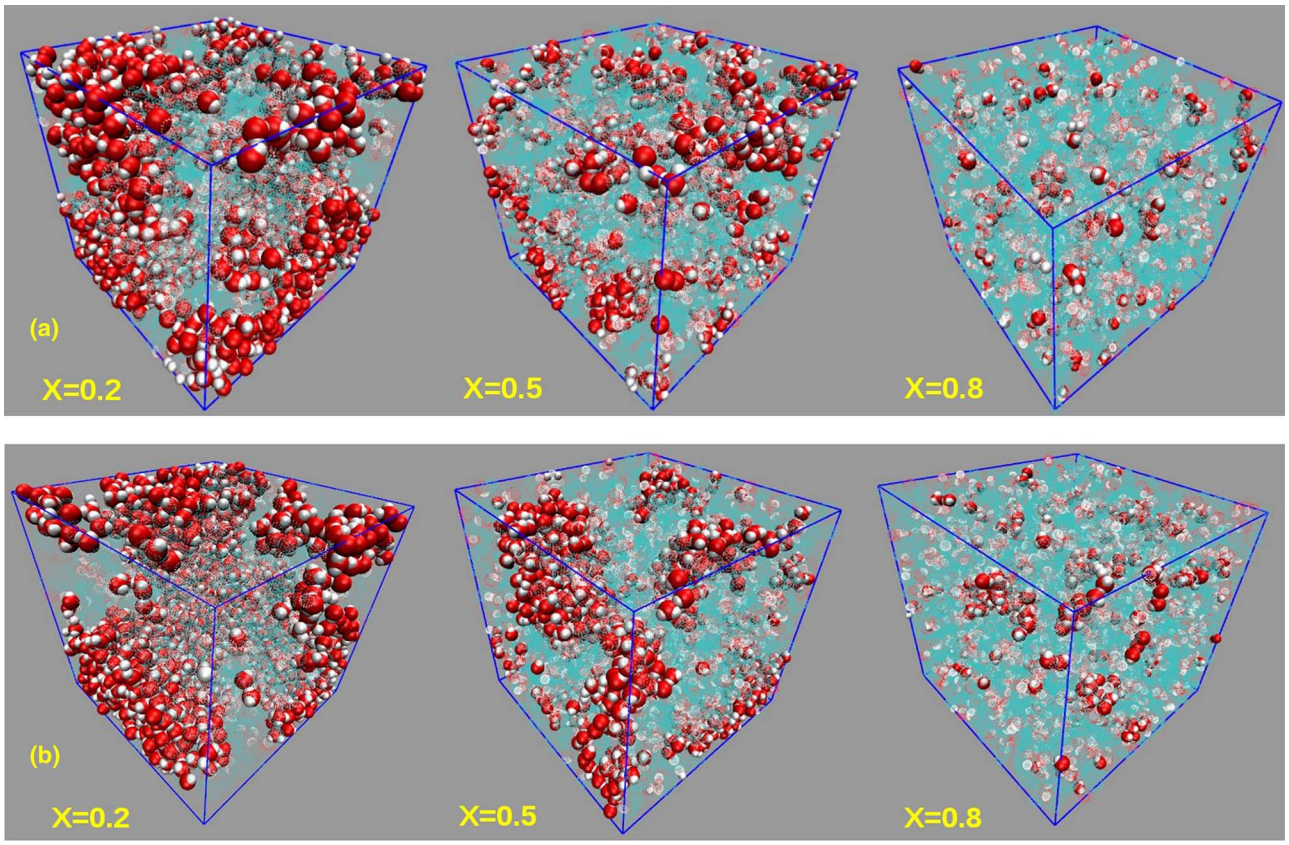

FIG. 3. (a) Snapshots for the OPLS TBA aqueous mixtures for three different TBA mole fractions. Water molecules are shown as red spheres for oxygen and white spheres for hydrogen. TBA is shown as semi-transparent molecule, with cyan sphere for oxygen and white spheres for hydrogen. (b) Snapshots for the TraPPE-UA TBA aqueous mixtures for three different TBA mole fractions. The conventions are as in (a).

differences that are better seen when looking at the excess quantities in the insets. Noting that these excess are about a percent or so of the original quantities, such small differences can acceptably represent the various inaccuracies of the models. In view of all the parameters that come into play, it is illusory to expect an agreement better than one percent. We will rather focus on the structural properties and the morphology of the mixture.

C. Snapshots

In Figs. 3(a) and 3(b), we show snaphots of the aqueous mixtures with the OPLS and TraPPE-UA force fields, respectively, at three typical mole fractions of TBA, $x = 0.2$, 0.5, and 0.8. We see that both models reproduce very similar micro-heterogeneous configurations for each mole fraction. The TraPPE-UA model induces a slightly larger clustering of water, which can be better observed by rotating the snapshots. These effects also show up in the KBI as we discuss below. In general, the mixtures look bi-continuous in the range $0.1 < x < 0.6$, and water forms small droplets or becomes mostly monomeric at low water contents.

D. Structure

In the first part, we examine structural features due to the micro-heterogeneity of the two mixtures through the analysis of the KBI. In the second part, we re-examine the same features through the underlying TS correction to the missing domain modulation due to finite size effects.

1. Kirkwood-Buff integrals

Figure 4 shows the various KBI – uncorrected by the TS extension, as obtained from the OPLS and TraPPE-UA models of TBA as well the previous OPLS results from Ref. 17. These latter results correspond to the original flexible OPLS with SPC water, so the results are expected to be slightly different from ours. The experimental results from Ref. 44 are equally shown as lines, and it is seen that the simulation results for a variety of force field combinations are all overestimating the experimental results by large factors. In view of the reasonable agreement, otherwise found for other thermodynamical properties, it is rather strange that such disagreement should occur for this particular property. In fact, such disagreement has been found several times before for different aqueous mixtures, and seems to be a recurrent and inherent feature in simulation of self-associating systems. The natural way to avoid this disagreement is to reformulate the force field parameters in order to bring the KBI to smaller values. It is not obvious that this operation can be performed, especially by keeping other properties in the same good agreement with experiments as the previous version of the model. However, this has been repeatedly proved to be possible.[15–17] It is relatively easy to get an insight at the origin of large KBI values: the

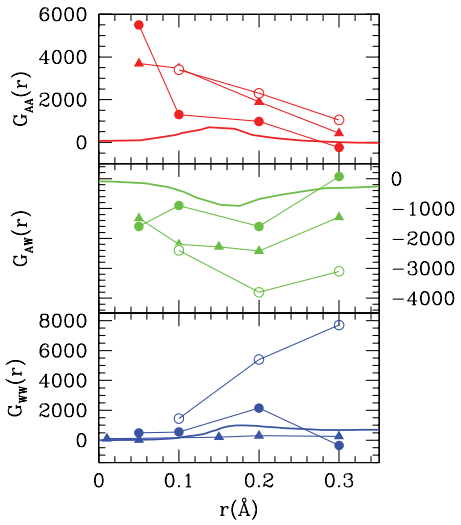

FIG. 4. Uncorrected KBI (symbols) from various TBA models versus TBA mole fraction x, compared to experimental ones (thick lines) from Ref. 44. The lines connecting the symbols are guidelines. Triangles from Ref. 17, open dots for the TraPPE-UA model and filled dots for the OPLS model.

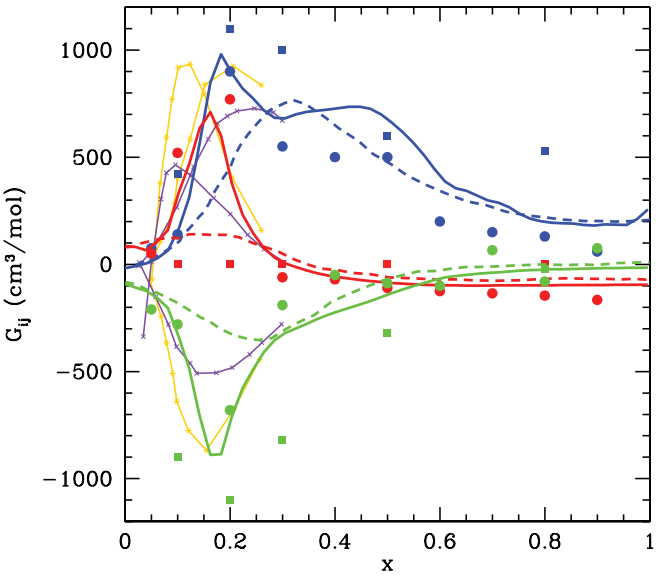

FIG. 5. Corrected KBI (symbols) from various TBA models versus TBA mole fraction x, compared to various experimental ones: continuous lines from Ref. 44, dashed lines from Ref. 45, magneta lines for SAXS data from Ref. 30 and cyan lines for SANS data from Ref. 44. Present calculations are shown in filled dots for the OPLS model and squares for the TraPPE-UA model. The color conventions are blue for G_{WW}, red for G_{AA}, and green for G_{WA}. Note that the SAXS and SANS data are undifferentiated (see text for more details).

micro-segregation in domains enhances the self-correlations between like species while reducing the cross-correlations between unlike species. As a result, the integral of the correlations acquire large values within the like-species domains, and smaller values in cross species correlations, due to the depletion of the adverse species. From this point of view, the enhanced KBI do appear as a natural feature to expect from micro-segregated systems. The problem is how to conciliate this expectation with the much smaller values observed in experiments. The route chosen by altering the solute force field amounts to decrease the micro-segregation such that the integrals acquire values smaller than the previous ones, and in better agreement with the experiments. The reason why this operation does not alter the thermodynamical properties such as enthalpy, for example, is due to the fact that the major contribution to these quantities comes from the short range correlations. If we accept that the original force fields do not require modifications, then we must accept the large domain sizes as a real feature. The only way this can be conciliated with experimental requirements is by modulating the correlations beyond those obtained from the simulations. This is the route we choose to illustrate here.

Figure 5 shows the KBI obtained from both OPLS and TraPPE-UA models after the TS extension has been implemented in the correlations, prior to integration. Also shown are the various experimental KBIs obtained from the calorimetry route and also the small-angle neutron scattering (SANS) and small-angle x-ray scattering (SAXS) route. These have been reported and discussed earlier in Ref. 44. In view of the large dispersion of the experimental results, we find that our TS-modified KBIs are now in reasonably good agreement with the experimental trends. In order to understand the dispersion of the experimental results, we need to look at the various ways of evaluating the KBI. The inversion of the Kirkwood-Buff approach allows one to express the KBI in terms of the compressibility κ_T, the volume V, and partial molar volumes V_W and V_A as well as the concentration fluctuation term $D = x(\partial\beta\mu_W/\partial x)_{PT}$, considered as a function of the TBA mole fraction x, as

$$G_{WA} = k_B T\kappa_T - \frac{V_W V_A}{V D},$$

$$G_{WW} = G_{WA} + \frac{1}{1-x}\left(\frac{V_W}{D} - V\right),$$

$$G_{AA} = G_{WA} + \frac{1}{x}\left(\frac{V_A}{D} - V\right).$$

The volumetric properties are in general well evaluated from experiments and are smooth looking. But the concentration fluctuation term D is generally obtained either from the experimentally obtained Gibbs free-energy,[45,46] or from the chemical potentials obtained by partial pressure measurements.[44,48] It is this term that is subject to large incertitudes or variations which in turn reflect through the dispersion of the various experimental KBIs. The exact reason as to why this is so, does not seem to have been clarified – to the best of our knowledge. It is interesting that different force fields differing between themselves by variations in force fields through details as small as few percents – as can be seen from Table I – can produce variations similar to those observed from the experimental KBI.

2. Teubner-Strey corrections

We now examine how the TS extension can rationalise the high apparent KBI obtained from the uncorrected RDFs. This is illustrated for alcohol–alcohol and water–water correlations through the site–site RDF $g_{OO}^{(A)}(r)$ between the TBA

TABLE I. Comparison between the force field parameters for TBA.

σ[Å]	CH_3	C	O	H
OPLS	3.91	3.8	3.07	0
TraPPE-UA	3.75	5.8	3.02	0
Ref. 17	3.75	6.64	2.95	0
ϵ[kJ/mol]				
OPLS	0.6699	0.2094	0.7117	0
TraPPE-UA	0.814	0.0415	0.7730	0
Ref. 17	0.8671	0.0070	0.8496	0
e(charge)				
OPLS	0	0.265	− 0.7	0.435
TraPPE-UA	0	0.265	− 0.7	0.435
Ref. 17	0	0.337	− 0.76	0.423

oxygen site and $g_{OO}^{(W)}(r)$ between the water oxygen sites, in Figs. 6 and 7 for $x = 0.2$ and Figs. 8 and 9 for $x = 0.8$. The top panel of each figure shows a zoom on the last part of the function obtained from simulations (as well as a zoom on the main peak part of the RDF in some cases). In Figs. 8 and 9, we show the importance of the LP correction by drawing the effective slope (in green) taken by the RKBI uncorrected for the LP effect mentioned in Sec. II E. The corrected RKBI appear more horizontal and tend to an asymptote that corresponds to the KBI. However, in many cases, the asymptote is not clear, and the TS extension allows us to fix the asymptote through the methodology explained above. It turns out that the parameters cannot be randomly chosen and come down to a very narrow range if one requires a continuity solution. This extension is shown in blue curves. When this extension is taken into account, the domain modulated oscillatory decay brings the RKBI to a new lower value of the asymptote that matches better the experimental values, as illustrated in the middle panels. In the case of $x = 0.8$, we show how the LP correction tends to distort the general oscillatory decay of the correlations, that produces a RKBI that oscillates around a tilted line, instead of the expected horizontal line. In many cases, the LP correction alone is sufficient to bring the RKBI to the correct asymptotes. In our calculations, we empirically found $d \approx 30$ Å and $\xi \approx 12$ Å for nearly all

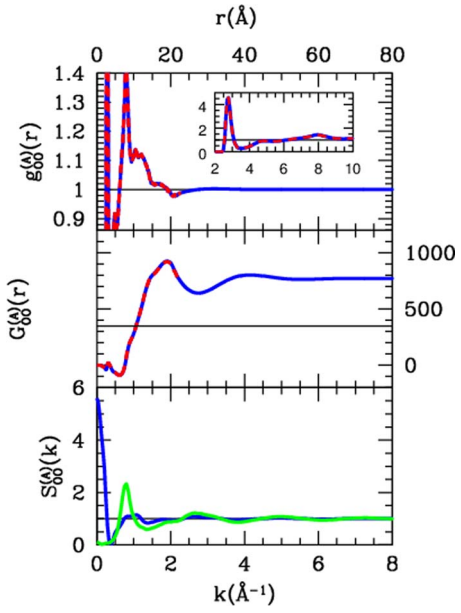

FIG. 6. Details of TS extension procedure for the OPLS TBA oxygen–oxygen correlations for the TBA mole fraction $x = 0.2$. Top panel, tail part of $g_{OO}^{(A)}(r)$ (the short range part shown in the inset): red dashed line for the uncorrected data, blue line after TS correction. Middle panel, RKBI $G_{OO}^{(A)}(r)$ with same line conventions as in top panel. Lower panel, structure factor $S_{OO}^{(A)}(k)$ with same line conventions as in top panel. The green curve is the structure factor of neat TBA.

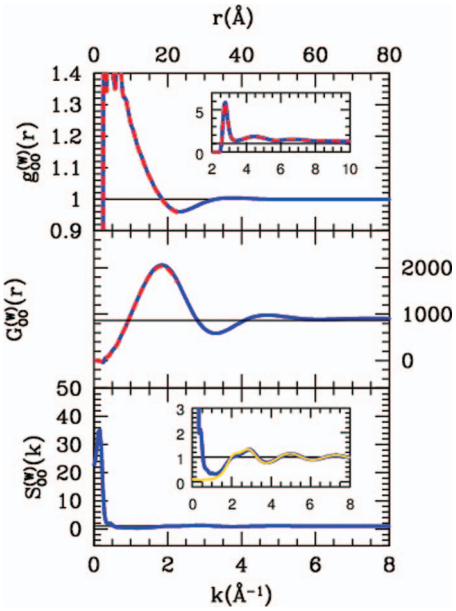

FIG. 7. Same as Fig. 6 but for water oxygen–oxygen correlations $g_{OO}^{(W)}(r)$ for $x = 0.2$. The gold curve in the inset of the lower panel is the structure factor of neat water.

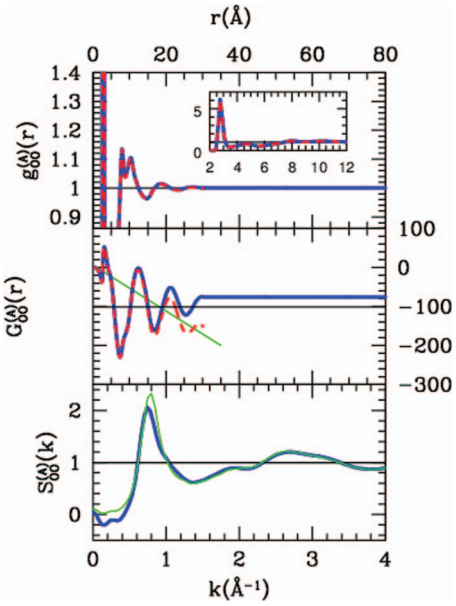

FIG. 8. Same as Fig. 6 but for $x = 0.8$. The green slanted line in the middle panel shows the wrong slope of the uncorrected data before the LP correction (see text). The green curve in the lower panel is the structure factor of neat TBA.

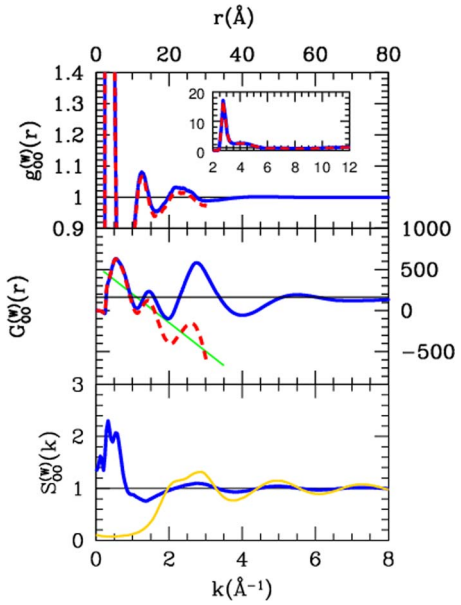

FIG. 9. Same as Fig. 7, but for $x = 0.8$. The green slanted line has same meaning as in Fig. 7. The gold curve in the lower panel is the structure factor of neat water.

concentrations in the range $x = 0.2 - 0.8$, where strong MH is observed, which tends to indicate that the long wavelength structure of the MH has the same topology. The TS extension is needed only when marked domains exist and can be seen in the snapshots. The lower panels show the structure factors, both the small-q range and the main peak range. We also show the neat liquid structure factors in order to appreciate how much the main peak changes. This is an indication on the nature and the extent of the micro-segregation: if the domains are large, then one can expect that the liquid structurally behaves as a neat liquid. This is not true, especially for water, where we see that the split main peak of neat water is often replaced by a single peak merging the two configurations of water in a single one. But the most spectacular feature of the structure factor is the pre-peak at small-q. This peak is generally noisy, because it is affected by the noise in the tail of RDFs. This is a typical TS pre-peak, that witnesses the existence of domains that modulate the decay of the molecular correlations.[7,9,10,41,47,49]

IV. DISCUSSION AND CONCLUSION

Micro-heterogeneous mixtures face two type of fluctuations: the genuine concentration fluctuations and the fluctuations in the size of domains that form the micro-heterogeneity. At first, it does not seem possible to separate one from the other if the domains are not well defined entities. This is particularly the case of aqueous mixtures of small polar solutes. To visualise this problem in a better way, let us consider a mixture of water with long alcohol chains which forms micelles in water. In such case, the micelles are well defined objects, and the fluctuations of their shape is something that can be unambiguously defined to some extent. Similarly, fluctuations in density of water between the micelles are easy to imagine. Now, when the micellar domains become smaller, they are less well defined, and it is harder to separate domain fluctuations from concentration fluctuations. Then, the question arises of how to represent such fluctuations and still keep the fact that the system is marked by domain formation. The answer that we give here is through the long range part of the correlation functions and the associated small-q behaviour of the structure factors.

We have demonstrated that the TS extension can bring to lower values the unphysically high KBI obtained by existing force fields. The question remains as to which of the two methods – altering the force fields or applying a TS extension – is the most appropriate. It all comes down to the question of the genuine extension of the micro-segregation in aqueous mixtures, or associated liquid mixtures in general. The micro-segregation is an intrinsic property of these systems. When we simulate such systems, we should adapt the size of simulation box in order to accommodate enough representations of the segregated domains, hence providing sufficient statistics on the decay of the correlations. There is no reason why a few thousands of molecules should represent the upper bound to simulate solutions. On the other hand, the methodology of altering the solute force field to fit the decay of RDFs within a box of a few thousand molecules seems to enforce the idea that usual simulation methods are still adequate for these systems. Very large scale simulations of unmodified force fields[52] are only likely to show the validity of the TS extension. It will not disprove the method of altering the force fields to suit smaller size simulations. We happen to think that this is a real problem for which we have no deciding criterion at the present stage of investigations. These two approaches can be viewed in analogy to the two ways of describing ionic solutions. One such way is to replace the long range Coulomb interactions by screened Yukawa-Debye-Huckel short range interactions, thus neglecting the presence of the solvent. This seems to bear some analogy to the methodology of altering the force fields in order to scale the micro-heterogeneity into the small-size system. The other way is to use an explicit solvent description with full scale Coulomb interactions. Such methodology is more expensive and also more sensitive to force field details, and the screened interactions should be recovered as a consequence of this detailed description. Following this line, one could use a reaction field method where long range interactions are not described beyond a certain range. We think that the TS methodology is akin to such description of the micro-heterogeneity. This analogy is only descriptive, and we expect to eventually capture this argument more properly into a statistical mechanic description of aqueous mixtures.

In a recent investigation,[53] we proposed a simple model of aqueous mixture, when SPC/E water is mixed with a "weaker" version of water obtained by scaling down the partial site charges of the SPC/E model. Such models exhibit a variety of micro-heterogeneity and can be considered as model molecular emulsions. In particular, it was shown through a very large system study ($N = 19\,384$) that such models do develop domain modulation through fluctuating clustering, and that the TS extension captures this feature quite nicely with simulations of smaller systems of $N = 2048$.

In Fig. 10, we compare the short range features of the RDFs from the two mixture models studied here with that

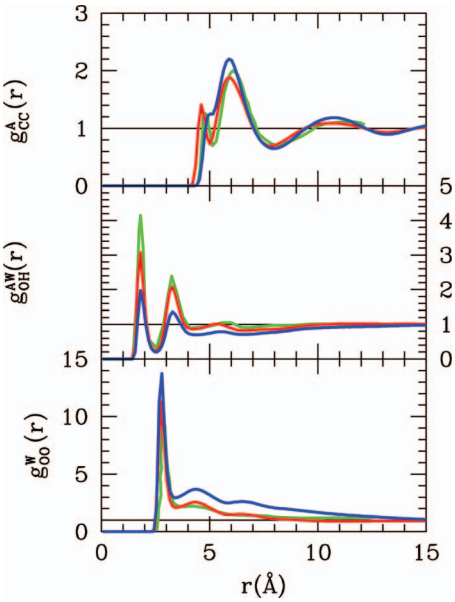

FIG. 10. Selected site–site RDFs for $x = 0.5$. Top panel: TBA–TBA correlations through carbon–carbon $g_{CC}(r)$. Middle panel water-TBC cross correlations through TBA oxygen and water hydrogen $g_{OH}(r)$. Lower panel water–water correlations through oxygen–oxygen $g_{OO}(r)$. Red for the OPLS, blue for the TraPPE-UA mixture models of present work, and green for the mixture model of Ref. 17.

from Ref. 17, the latter which alters the force field in order to reproduce the proper KBI within current system sizes. Various site–site correlations are examined, and it is clearly seen that all model combinations reproduce very similar features. It is rather surprising that the present OPLS model, that has the largest unmodified KBI (see Fig. 4), hence the largest micro-heterogeneity, is also very close to that of Ref. 17, which has the smallest micro-heterogeneity. The difference resides in the medium to long range features of the RDFs, as seen in the lower panel for the water-water RDF $g_{OO}(r)$: the correlations drop below 1 after 8 Å for the mixture model of Ref. 17, which brings the KBI to more modest values. The TraPPE-UA model clearly overestimates the domain correlations as compared to the two others.

In order to decide between the two approaches we need a criterion from the experimental side. For example, the clear unambiguous demonstration of the existence of the pre-peak will confirm the present picture, while its absence will validate the approaches that reduce the micro-heterogeneity by altering the force field of the solute. There are two such data available, on one hand from neutron scattering measurements in Refs. 12, 27, and 28 and on the other hand from SAXS measurements in Refs. 29 and 30. In the first set of references, it is very hard to tell from the scale of the plots if there is a possibility for a pre-peak at very small k-vectors. The second set of references produce small-k plots explicitly, and some small-k behaviour in Ref. 29 plotted in log-scale look like there could be a weak pre-peak at $k \approx 0.015$ Å^{-1} for $x = 0.085$. From the look of some of these scattering data, aqueous TBA could be in the Lifshitz state, a state often found in micro-emulsions, where the pre-peak is just emerging from $k = 0$.[47,49] The rather large pre-peak observed in the present simulations could be an artifact of the present classical models. It is unfortunate that the available experimental data are not solid enough to make firm conclusions about the conjecture of the present work. It may be worth noting that aqueous-TBA was quoted by several authors as being highly inhomogeneous, with possible clathrate-like sub-structure.[54–56]

ACKNOWLEDGMENTS

This work shows that simple solutions, known for decades from experimental point of view, and possibly thought to be fully understood from simulation point of view, hide new mysteries to explore, hence are worthwhile re-investigating.

[1] *Micellization, Solubilization, and Micro-emulsions*, edited by K. W. Mittal (Plenum, New York, 1977).
[2] A. M. Cazabat, D. Langevin, J. Meunier, and A. Pouchelon, J. Phys. Lett. **43**, 89 (1982).
[3] J. Frölich, Lect. Notes Phys. **216**, 31 (1985).
[4] G. Gomper and M. Schick, Phys. Rev. Lett. **62**, 1647 (1989).
[5] T. M. Teubner and J. Strey, J. Chem. Phys. **87**, 3195 (1987).
[6] *Principle of Condensed Matter Physics*, edited by P. M. Chaikin and T. C. Lubensky (Cambridge University Press, 2000).
[7] R. Strey, Colloid Polym. Sci. **272**, 1005 (1994).
[8] M. A. Floriano, E. Caponetti, and A. Z. Panagiotopoulos, Langmuir **15**, 3143 (1999).
[9] G. D'Arrigo, R. Giodano, and J. Teixeira, Eur. Phys. J. E **10**, 135 (2003).
[10] G. D'Arrigo, R. Giodano, and J. Teixeira, Eur. Phys. J. E **29**, 37 (2009).
[11] S. Dixit, J. Crain, W. C. Poon, J. L. Finney, and A. K. Soper, Nature (London) **416**, 829 (2002).
[12] D. T. Bowron, J. L. Finney, and A. K. Soper, J. Phys. Chem. **102**, 3551 (1998).
[13] S. K. Allison, J. P. Fox, R. Hargreaves, and S. P. Bates, Phys. Rev. B **71**, 024201 (2005).
[14] T. Delmas, H. Piraux, A.-C. Couffin, I. Texier, F. Vinet, P. Poulin, M. E. Cates, and J. Bibette, Langmuir **27**, 1683 (2011).
[15] E. A. Ploetz, N. Bentenitis, and P. E. Smith, Fluid Phase Equilib. **290**, 43 (2010).
[16] S. Weerasinghe and P. E. Smith, J. Chem. Phys. **118**, 10663 (2003).
[17] M. E. Lee and N. F. A. van der Vegt, J. Chem. Phys. **122**, 114509 (2005).
[18] A. Perera and F. Sokolić, J. Chem. Phys. **121**, 22 (2004).
[19] J. C. Berendsen, J. P. M. Postma, W. F. Von Gusteren, and J. Hermans, in *Intermolecular Forces*, edited by B. Pullman (Reidel, Dortrecht, 1981).
[20] W. L. Jorgensen, "Optimized intermolecular potential functions for liquid alcohols," J. Phys. Chem. **90**(7), 1276–1284 (1986).
[21] B. Chen, J. J. Potoff, and J. I. Siepmann, J. Phys. Chem. B **103**, 3093 (2001).
[22] A. Baranowski, K. Jerie, and J. Glinksky, Chem. Phys. **214**, 143 (1997).
[23] T. M. Bender and R. Pecora, J. Phys. Chem. **90**, 1700 (1986).
[24] K. Iwasaki and T. Fujiyama, J. Phys. Chem. **83**, 463 (1979).
[25] H. Tanaka, K. Nakanishi, and H. Touhara, J. Chem. Phys. **81**, 4065 (1984).
[26] P. G. Kusalik, A. P. Lyubartsev, D. L. Bergman, and A. Laaksonen, J. Phys. Chem. B **104**, 9533 (2000).
[27] D. T. Bowron, A. K. Soper, and J. L. Finney, J. Chem. Phys. **114**, 6203 (2001).
[28] D. T. Bowron and S. Diaz-Moreno, J. Chem. Phys. **117**, 3753 (2002).
[29] H. D. Bale, R. E. Shepler, and D. K. Sorgen, Phys. Chem. Liq. **1**, 181 (1968).
[30] K. Nishikawa, Y. Kodera, and T. Iijima, J. Phys. Chem. **91**, 3694 (1987).
[31] L. Blum and A. J. Torruela, J. Chem. Phys. **56**, 303 (1972).
[32] P. H. Fries and G. N. Patey, J. Chem. Phys. **82**, 429 (1985).
[33] P. G. Kusalik and G. N. Patey, J. Chem. Phys. **88**, 7715 (1988).
[34] J. P. Hansen and I. R. McDonald, *Theory of Simple Liquids* (Academic, London, 1986).
[35] M. E. Fisher, J. Math. Phys. **5**, 944 (1964).
[36] A. Perera and G. N. Patey, J. Chem. Phys. **89**, 5861 (1988).
[37] DL_POLY package, CCLRC Daresbury Laboratory, see http://www.cse.clrc.ac.uk.

[38]A. Perera, L. Zoranić, F. Sokolić, and R. Mazighi, J. Mol. Liq. **159**, 52 (2011).
[39]J. L. Lebowitz and J. K. Percus, Phys. Rev. **122**, 1675 (1961).
[40]M. Mijaković, B. Kežić, L. Zoranić, F. Sokolić, A. Asenbaum, C. Pruner, E. Wilhelm, and A. Perera, J. Mol. Liq. **164**, 66 (2011).
[41]A. Perera, B. Kežić, F. Sokolić, and L. Zoranić, in *Molecular Dynamics*, edited by L. Wang (InTech, Rijeka, 2012), Vol. 2.
[42]R. Wedberg, J. P. O'Connell, G. H. Peters, and J. Abildskov, Mol. Simul. **36**, 1243 (2010).
[43]L. Zoranić, R. Mazighi, F. Sokolić, and A. Perera, J. Chem. Phys. **130**, 124315 (2009).
[44]A. Perera, F. Sokolic, L. Almasy, P. Westh, and Y. Koga, J. Chem. Phys. **123**, 024503 (2005).
[45]E. Matteoli and L. Lepori, J. Chem. Phys. **80**, 2856 (1984).
[46]Y. Marcus, Monatsch. Chem. **132**, 1387 (2001).
[47]R. D. Koehler, K. V. Schubert, R. Strey, and E. W. Kaler, J. Chem. Phys. **101**, 10843 (1994).
[48]Y. Koga, *Solution Thermodynamics and its Application to Aqueous Solutions* (Elsevier, Amsterdam, 2007).
[49]A. Ciach and W. T. Gozdz, Annu. Rep. Prog. Chem., Sect. C; Phys. Chem. **97**, 269 (2001).
[50]Y. Koga, W. W. Y. Siu, and T. Y. H. Wong, J. Phys. Chem. **94**, 7700 (1990).
[51]K. Nakanishi, N. Kato, and M. Maruyama, J. Phys. Chem. **71**, 814 (1967).
[52]R. Gupta and G. N. Patey (unpublished).
[53]A. Perera, R. Mazighi, and B. Kežić, J. Chem. Phys. **136**, 174516 (2012).
[54]T. M. Bender and R. Pecora, J. Phys. Chem. **90**, 1700 (1986).
[55]D. T. Bowron and J. L. Finney, J. Phys. Chem. **111**, 9838 (2007).
[56]D. Subramanian, D. A. Iganov, I. K. Yudin, M. A. Anisimov, and J. V. Sengers, J. Chem. Eng. Data **56**, 1238 (2011).